ELSEVIER

Chemical Geology 152 (1998) 211–225

CHEMICAL GEOLOGY
INCLUDING
ISOTOPE GEOSCIENCE

Raman spectra of potassium carbonate and bicarbonate aqueous fluids at elevated temperatures and pressures: comparison with theoretical simulations

John D. Frantz *

Geophysical Laboratory, Carnegie Institution of Washington, Washington, DC 20015, USA

Received 15 October 1997; revised 17 May 1998; accepted 17 May 1998

Abstract

One-molal solutions of potassium carbonate and potassium bicarbonate were investigated by Raman spectroscopy from 22° to 550°C and from 1000 to 2000 bar. Experiments were performed in a special hydrothermal pressure vessel fitted with conical diamond windows. Frequencies and half-widths of the vibrational modes were measured for both carbonate and bicarbonate as a function of temperature and pressure. In the case of potassium carbonate solutions, dissolved bicarbonate appeared with its concentration dramatically increasing with increasing temperature and decreasing density. The opposite behavior occurred in the case of potassium bicarbonate: the relative concentration of dissolved carbonate increased relative to total bicarbonate. In addition, at temperatures above 300°C, dissolved aqueous carbon dioxide appeared with its concentration continuing to increase with increasing temperature and decreasing density. Simulations using theoretically-predicted mass action constants were used to compute changes in solution speciation for these solutions as they were subjected to increased temperature and pressure. Results resulting from these predictions matched those discovered in the spectral measurements.

Keywords: Potassium carbonate; Potassium bicarbonate; Raman spectroscopy

1. Introduction

The composition of natural high-temperature, high-pressure fluids in the Earth's crust have a significant influence on the evolution and resulting mineral paragenesis of igneous and metamorphic rock suites. Of particular interest are fluids containing C–O–H gas mixtures due to the frequent occurrence of carbon dioxide and methane in hydrothermal fluids and the common presence of carbon-bearing minerals in associated rock suites. These fluids, mixtures of gases, dissolved electrolytes and water, exist either as a single supercritical phase or as a mixture of two immiscible phases (Zhang and Frantz, 1989, 1992). Though considerable effort has been devoted towards understanding gas equilibria in this system (Eugster and Skippen, 1967; Greenwood, 1969, 1973; Kerrick and Jacobs, 1981; Holloway,

* Fax: +1 202 686 2419; e-mail: frantz@gl.ciw.edu

0009-2541/98/$ - see front matter
PII: S0009-2541(98)00058-8

Table 1
Solution compositions of one-molal potassium carbonate and one-molal potassium bicarbonate at 25°C, 1 atm

Species	K_2CO_3	$KHCO_3$
$KOH^{\cdot}$	1.47×10^{-3}	1.67×10^{-7}
K^+	1.49×10^{0}	9.27×10^{-1}
OH^-	5.37×10^{-3}	1.04×10^{-6}
H^+	3.74×10^{-12}	2.05×10^{-8}
HCO_3^-	6.08×10^{-3}	8.96×10^{-1}
CO_3^{2-}	5.36×10^{-1}	1.19×10^{-2}
CO_2 (aq)	2.50×10^{-8}	1.92×10^{-2}
KCO_3^-	4.06×10^{-1}	6.80×10^{-3}
$K_2CO_3^{\cdot}$	5.10×10^{-2}	4.96×10^{-4}
$KHCO_3^{\cdot}$	7.62×10^{-4}	6.54×10^{-2}

1984; Saxena and Fei, 1988), little attention has been devoted towards the investigation of the relative concentrations of dissolved carbon-bearing electrolytes. The complexity of experimentally investigating such fluids is due to: (1) their dependence on oxidation fugacity; (2) the number of mass action constants needed to describe the system; and (3) the low solubilities of many of the salts. To address these difficulties, a combined experimental and theoretical approach has been adopted using in-situ spectroscopic measurements in combination with predictive thermochemical calculations on relatively soluble solutions in the potassium carbonate–water system. Such solutions are amenable to Raman studies and can serve to test the theoretically-predicted mass-action constants used to describe the distribution of dissolved species in carbonate-bearing fluids.

Davis and Oliver (1972) in their study of potassium carbonate solutions described the Raman spectra of aqueous carbon dioxide, bicarbonate and carbonate ions at room temperature and pressure. They demonstrated the presence of a limited amount of interaction between molecular carbon dioxide and water with only minor amounts of CO_2 existing as H_2CO_3. They deciphered the vibrational symmetries

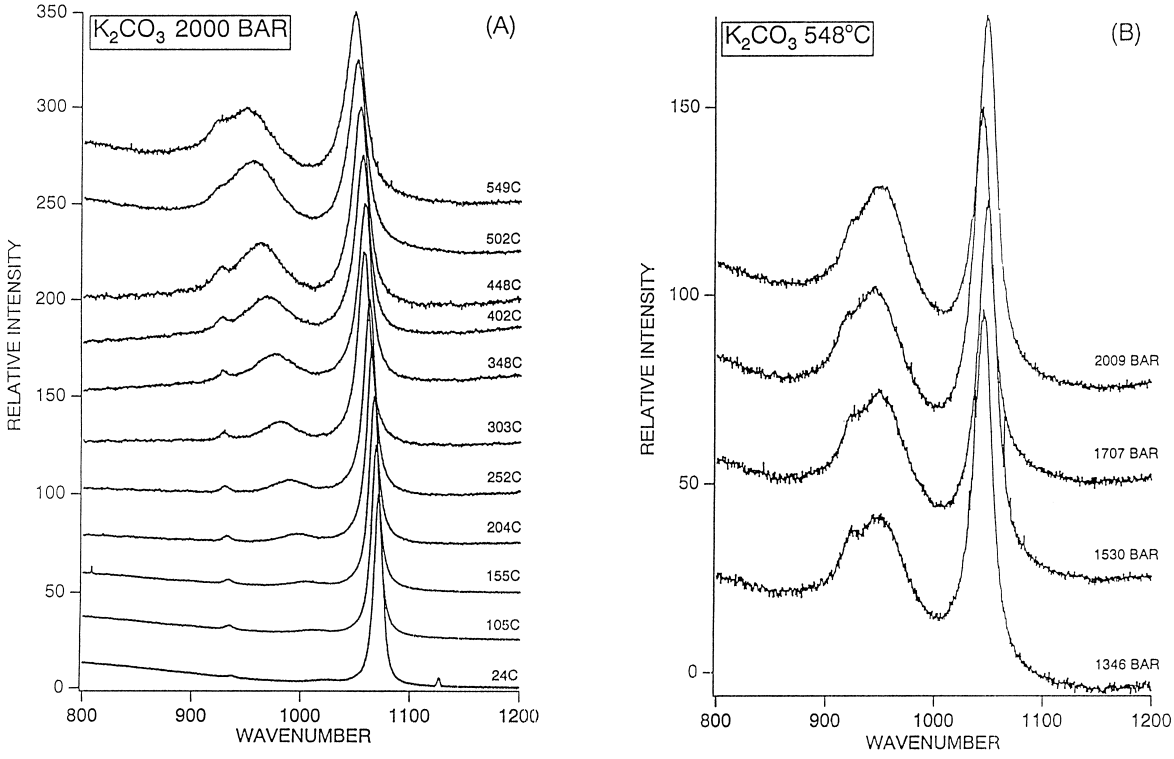

Fig. 1. Raman spectra of aqueous one-molal potassium carbonate solutions. (A) Spectra collected at varying temperatures at 2000 bar. (B) Spectra collected at 548°C at varying pressures.

of the bicarbonate and carbonate ions, suggested that small amounts of carbonate coexist with bicarbonate in potassium bicarbonate solutions and demonstrated the dependence of the ratio of dissolved carbonate to bicarbonate on pH. Oliver and Davis (1973) investigated the vibrational spectra of bicarbonate and carbonate solutions containing lithium, sodium, potassium, rubidium, and cesium at room temperature and pressure. They demonstrated that carbonate and bicarbonate spectra at 25°C, 1 atm are independent of concentration and the alkali metal and thus saw no evidence of ion-pairing. Kruse and Franck (1982) investigated two molar potassium bicarbonate solutions to 300°C suggesting that increased abundances of carbonate might be forming at the expense of bicarbonate with increasing temperature. They also determined the presence of bicarbonate ions in 3% CO_2–H_2O mixtures at 34°C, 750 bar. Dubessy et al. (1997) investigated the behavior of carbon dioxide–water mixtures using synthetic fluid inclusions. Evidence of molecular interactions between carbon dioxide and water were documented under hydrothermal conditions.

2. Experimental methods

The Raman spectra of potassium carbonate- and bicarbonate-bearing aqueous solutions were collected

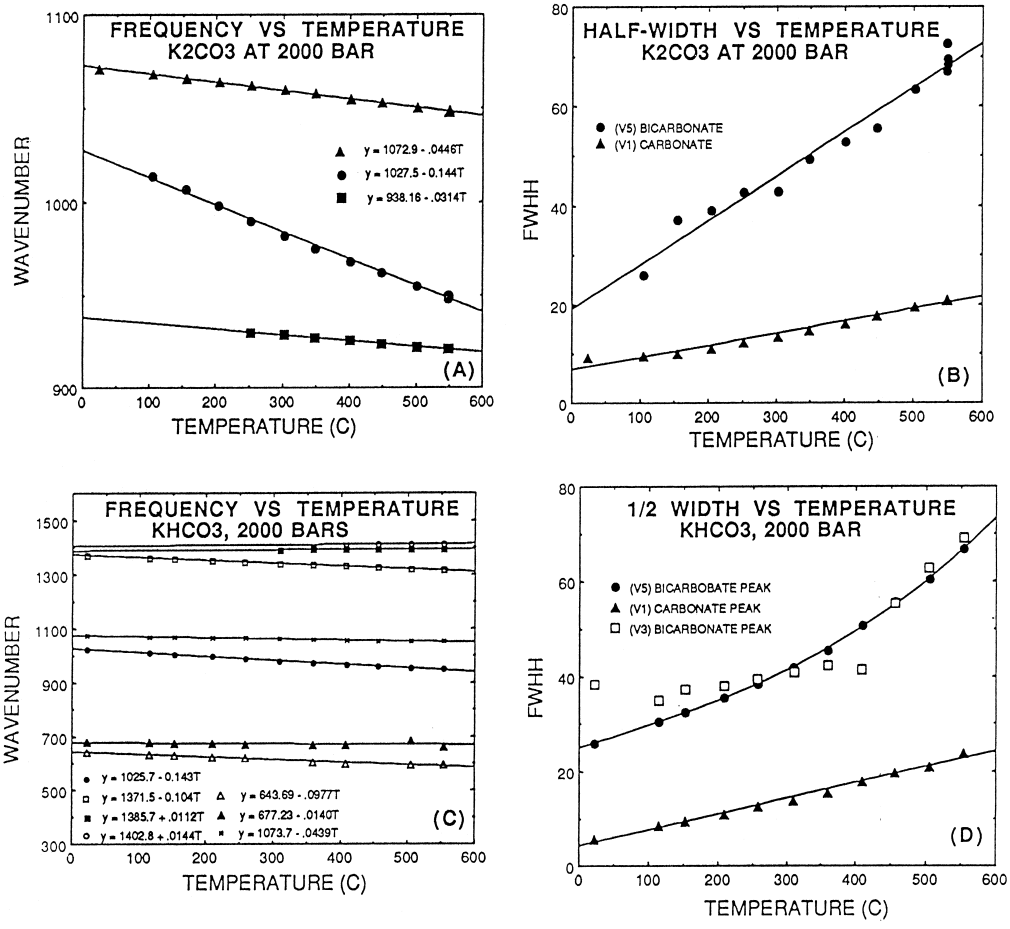

Fig. 2. Peak frequencies and half-widths as a function of temperature at 2000 bar for one-molal potassium carbonate and potassium bicarbonate solutions.

using a specially-designed hydrothermal pressure vessel with diamond windows (Frantz, 1981; Frantz et al., 1993). The disk-shaped pressure vessel (diameter: 2 in.; height: 1 in.) contains two conical low-fluorescence diamond windows set at right angles to one another. The cell, containing a $Pt–Pt_{90}Rh_{10}$ thermocouple extending into the fluid cavity, is heated using two spirally-wound platinum resistance furnace elements. The fluid is introduced and pressure is generated using a small stainless-steel intensifier. Pressure is measured using an Autoclave® 0–60 000 psi transducer. Pressure calibration of the transducer was accomplished using a recently calibrated Heise® bourdin-tube gauge. A melting point furnace was used in the temperature calibration of the thermocouples. Temperature errors are thought to be ± 5°C; pressure errors, ± 10 bar. The pressure vessel and much of the pressure-generating apparatus are gold plated to reduce the effects of corrosion and therefore inhibit fluorescence. Prior to use, the cell and associated pressure-generating apparatus were repeatedly cleaned with ultra-pure hexane, methanol, and triple-distilled water. Great care was taken in filling the system with the sample fluid in order to prevent the introduction of dust and bubbles.

The optical cell was used in conjunction with a Dilor® XY confocal Raman spectrometer equipped with an intensified diode array detector. Gratings with 1800 lines/mm yield a spectral resolution of approximately 1 cm^{-1}. The 514.5 nm line of a SpectroPhysics® model 2025 Ar^{+} laser operating at 1.8 W was used for sample excitation. The spectrometer was calibrated with respect to wavenumber using both the frequency of the laser line and a mercury lamp. Collection of the scattered light was at 90°C to the incident radiation. Experiments were performed by first incrementing temperature and measuring spectra at varying pressures. Signal collection times averaged 300 seconds. Analyses of the resulting Raman spectra were accomplished using computer algorithms contained in the software package Igor Pro (WaveMetrics®).

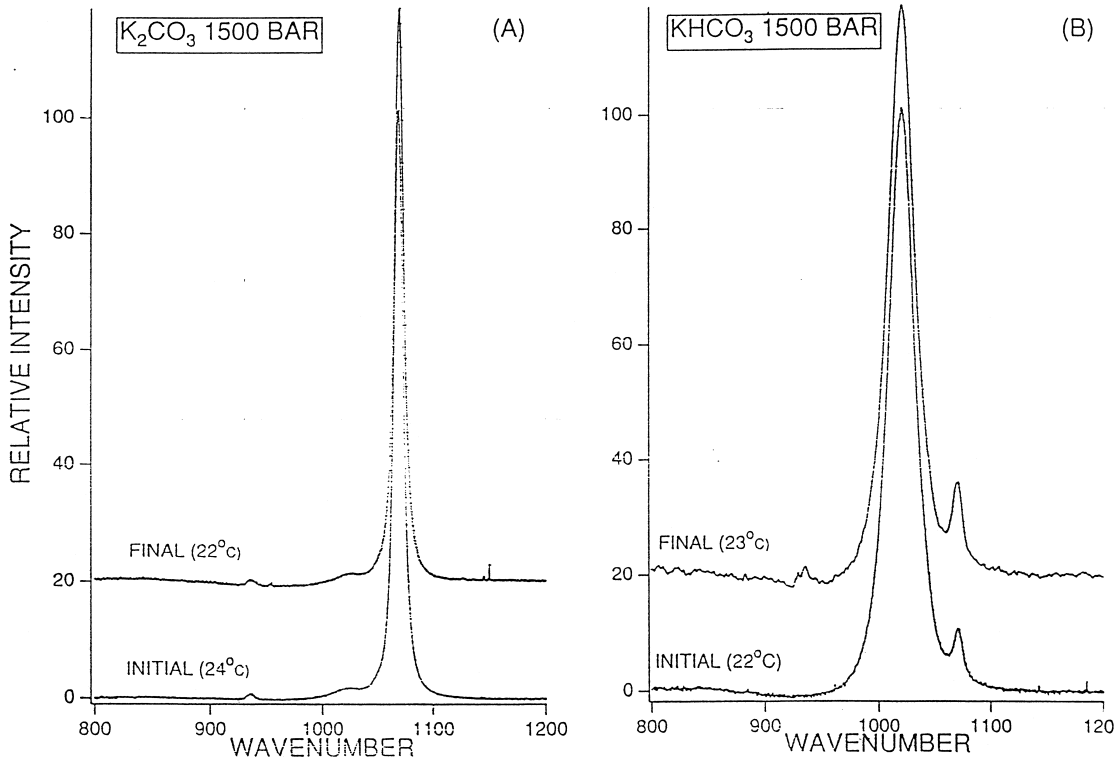

Fig. 3. Comparison of Raman spectra taken at standard temperature at 1500 bar before and after high temperature measurements. (A) Potassium carbonate; (B) Potassium bicarbonate.

The one-molal potassium carbonate aqueous solution was prepared from granular anhydrous potassium carbonate reagent (Alfa®, Lot No. 010686) and doubly-distilled water; the one-molal potassium bicarbonate solution, from granular potassium hydrogen carbonate (Aldrich®, Lot No. 06930AQ). The concentration of both solutions were verified after preparation by analysis of potassium using atomic absorption spectrometry. No effort was made to degas or equilibrate the solution with atmospheric carbon dioxide.

3. Experimental results

Potassium carbonate in binary K_2CO_3–H_2O aqueous solutions exists primarily as potassium and carbonate ions under standard temperature and pressure conditions (Table 1). Values of pH are calculated to be in the range of 11.4 though they were not measured. There is, however, a small abundance of bicarbonate ions. The isolated carbonate ion (D_{3h} symmetry) exhibits four fundamental modes of vibration (Davis and Oliver, 1972). Of these, only

Table 2
Spectral parameters. One-molal potassium carbonate solution

T (°C)	Pressure (bar)	Carbonate (ν_1)			Bicarbonate (ν_5)			920 Peak	Mole fraction	
		Frequency	Area	FWHH	Frequency	Area	FWHH	Frequency	HCO_3	CO_3
24	2009	1071.0	1321	9.1	NA	NA	NA	NA	NA	NA
24	1522	1070.8	1330	9.0	NA	NA	NA	NA	NA	NA
24	1019	1070.5	1348	8.9	NA	NA	NA	NA	NA	NA
105	2004	1068.4	1324	9.6	1011.9	NA	15.3	NA	0.011	0.989
105	1539	1068.1	1286	9.7	1010.5	NA	24.5	NA	0.026	0.974
105	1039	1067.8	1286	9.7	1008.7	NA	10.9	NA	0.007	0.993
155	2015	1066.5	1295	10.2	1003.6	NA	18.0	NA	0.022	0.978
155	1490	1066.1	1205	10.4	1002.4	NA	12.8	NA	0.015	0.985
154	1061	1065.8	1121	10.6	1000.5	NA	17.1	NA	0.020	0.980
204	2008	1064.4	1172	11.2	996.2	NA	19.3	NA	0.040	0.960
201	1511	1064.0	1035	11.2	995.3	NA	18.8	NA	0.042	0.958
203	1059	1063.7	864	11.4	994.2	NA	18.2	NA	0.046	0.954
252	2020	1062.1	1068	12.3	990.0	265	42.7	930.1	0.199	0.801
252	1528	1061.7	922	12.2	988.4	185	36.2	930.1	0.167	0.833
253	1036	1061.3	792	12.5	987.3	154	34.8	929.3	0.162	0.838
303	2018	1059.9	919	13.5	982.0	333	42.8	928.6	0.266	0.734
301	1529	1059.5	835	13.5	981.4	235	37.8	928.4	0.220	0.780
301	1064	1059.0	759	13.6	980.1	194	35.4	928.0	0.203	0.797
348	1996	1057.7	866	14.8	974.9	472	49.2	927.4	0.353	0.647
350	1512	1057.3	821	14.9	974.0	346	42.5	927.6	0.296	0.704
351	1018	1056.8	775	15.0	972.5	355	45.1	927.3	0.315	0.685
402	2016	1055.2	912	16.2	968.0	681	52.8	925.7	0.427	0.573
399	1522	1054.8	912	16.2	966.7	585	49.2	926.3	0.391	0.609
399	1045	1054.3	936	16.3	965.5	647	52.8	925.7	0.409	0.591
448	2043	1053.1	877	17.7	962.0	839	55.6	924.0	0.489	0.511
448	1545	1052.6	1015	18.0	961.3	859	54.7	924.5	0.458	0.542
448	1052	1052.1	1065	17.8	959.6	765	52.1	924.5	0.418	0.582
502	2019	1050.4	1737	19.4	955.3	2231	63.3	922.1	0.562	0.438
508	1527	1049.6	1761	19.1	953.1	2230	66.2	921.0	0.559	0.441
508	1041	1049.0	1677	19.2	949.2	1826	66.7	942.3	0.521	0.479
549	2009	1048.7	1690	20.8	950.3	2516	68.4	920.9	0.598	0.402
548	1709	1048.3	1662	20.7	950.1	2214	66.9	921.2	0.571	0.429
549	1530	1048.1	1610	20.7	948.8	2114	69.4	920.7	0.568	0.432
548	1346	1047.7	1568	20.7	948.2	1981	72.5	920.8	0.558	0.442

NA = not analyzed.
FWHH = full width at half height.

three are Raman active. The principal mode, the symmetric stretch $\nu_1(A'_1)$ occurs at 1064 cm^{-1}. The modes $\nu_3(E')$ and $\nu_4(E')$ occur at 1436 (1380) cm^{-1} and 684 cm^{-1}, respectively. Interaction between potassium and carbonate if associated as ion pairs at standard temperature and pressure would not be Raman active due to the ionic nature of their bond.

Binary solutions of $KHCO_3$–H_2O, on the other hand, contain primarily potassium and bicarbonate ions at standard temperature and pressure (Table 1). Values of pH are in the range of 7.7; potassium bicarbonate solutions appear to contain minor amounts of carbonate ions. Assuming the $C_s(\sigma_h)$ symmetry model (Davis and Oliver, 1972), nine fundamental modes of vibration exist for the bicarbonate ion. Of these an intense C–OH stretching mode ($\nu_5(A')$) is present at 1017 cm^{-1}. Bands representing the (OH)CO bending mode ($\nu_7(A')$) and the CO_2 bending mode ($\nu_6(A')$) are at 632 and 672 cm^{-1}, respectively. The COH bending mode ($\nu_4(A')$) is at 1302 cm^{-1} and the symmetric CO stretch ($\nu_3(A')$) is at 1360 cm^{-1}.

Potassium carbonate and potassium bicarbonate solutions at standard temperatures and pressures (Table 1) contain only minor molal amounts of aqueous carbon dioxide (2.5×10^{-8} and 1.9×10^{-2}, respectively). Molecular carbon dioxide, $D_{\infty h}$ symmetry, exhibits three fundamental vibrational modes: a symmetric stretching mode (ν_1); a doubly degenerate bending mode (ν_2); and an antisymmetric stretching mode (ν_3). Of these, only the symmetric stretching mode is Raman active. Carbon dioxide does, however, exhibit Fermi resonance due to the interaction of the Raman-active overtone of the bending mode (ν_2) with the fundamental stretching mode (ν_1) resulting in the fermi diad with peaks at 1388 and 1285 cm^{-1} (Colthup et al., 1975). In addition to the fermi diad, carbon dioxide at elevated temperatures

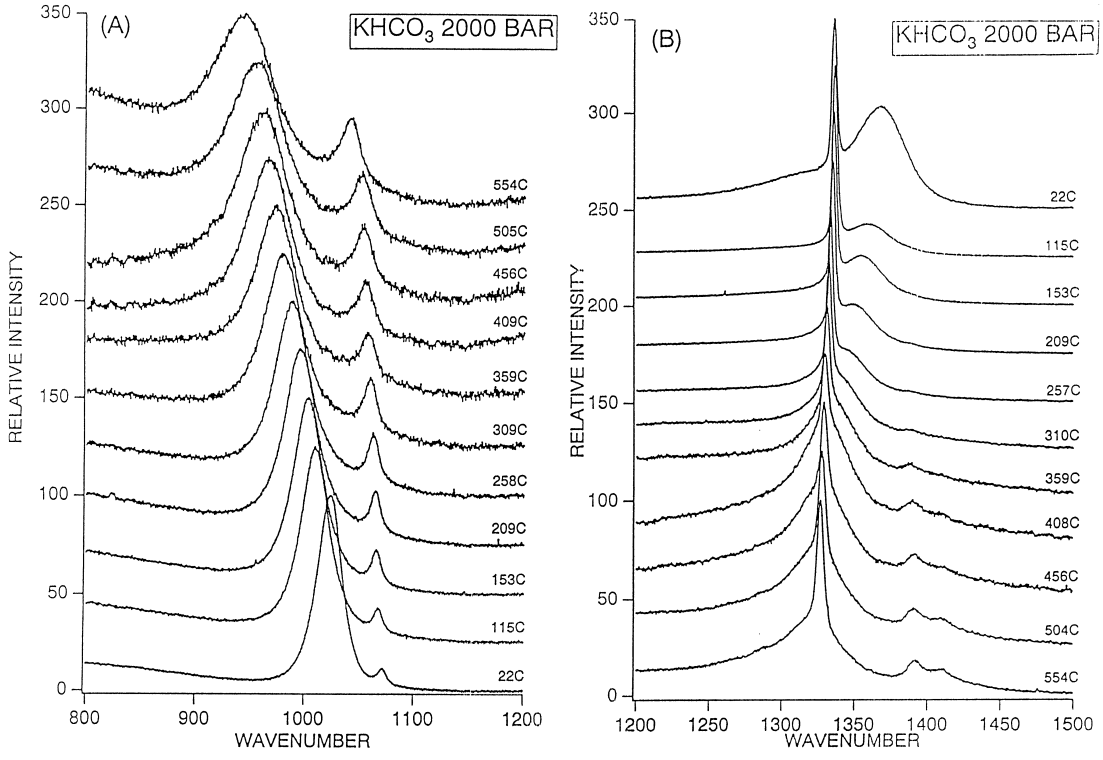

Fig. 4. Raman spectra of aqueous one-molal potassium bicarbonate solutions. (A) Spectra collected in the spectral range 800 to 1200 cm^{-1} at varying temperatures at 2000 bar. (B) Spectra collected in the spectral range 1200 to 1500 cm^{-1} at varying temperatures at 2000 bar.

and pressures exhibits 'hot bands' at frequencies below 1285 cm^{-1} and above 1388 cm^{-1} (Dubessy et al., 1997).

3.1. K_2CO_3

Raman spectra of a one-molal solution of potassium carbonate solution were collected in the optical cell at temperatures ranging from 24 to 549°C at approximately 50° intervals and at pressures of approximately 1000, 1500 and 2000 bar. The spectral range was between 710 and 1275 cm^{-1}. Portions of the resulting spectra taken at varying temperatures at 2000 bar are shown in Fig. 1(A). The most prominent feature of the spectra is the large peak with a midpoint at a frequency of 1071 cm^{-1} for the 24°C spectrum. The frequency of this band systematically decreases to 1048 cm^{-1} as temperature is increased to 549°C. This band represents the carbonate symmetric stretch ($\nu_1(A')$). The second feature evident in Fig. 1(A) is the peak located on the low-frequency shoulder of the $\nu_1(A')$ band. The frequency of this band systematically decreases from 1012 cm^{-1} at 105°C to 950 cm^{-1} at 549°C. The peak corresponds not to a carbonate mode, but to the C–OH stretching mode of the bicarbonate ion ($\nu_5(A')$). The third feature is a small peak decreasing from 935 cm^{-1} to 921 cm^{-1} as temperature is raised to 549°C. This feature appears to be the result of scattering from the pressure vessel itself as it occurs with the water blank. The variations in peak positions and their half-widths are shown in Fig. 2(A) and (B), respectively. Spectra, showing the same features, taken at 548°C at various pressures are shown in Fig. 1(B). Raman spectra taken both before and after the high-temperature measurements (Fig. 3(A)) indicate that the bulk solution composition remained unchanged during the experiments. A summary of the frequencies, 1/2 widths and integrated areas corresponding to these peaks for spectra taken at the various temperatures and pressures are given in Table 2.

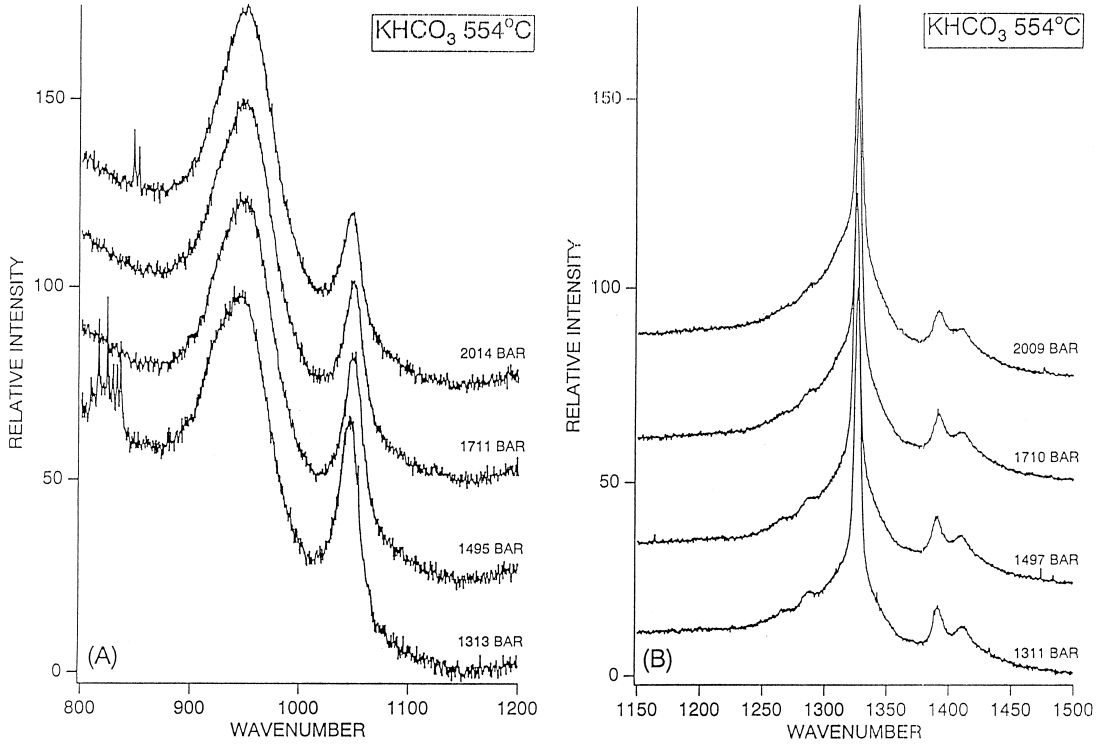

Fig. 5. Raman spectra of aqueous one-molal potassium bicarbonate solutions. (A) Spectra collected in the spectral range 800 to 1200 cm^{-1} at 554°C at varying pressures. (B) Spectra collected in the spectral range 1150 to 1500 cm^{-1} at 554°C at varying pressures.

3.2. $KHCO_3$

Raman spectra of a one-molal solution of potassium bicarbonate solution were collected at the same approximate temperature and pressure intervals as in the case of potassium carbonate. Three spectral ranges were studied: (1) 710–1275 cm^{-1}; (2) 1075–1614 cm^{-1}; and (3) 296–889 cm^{-1}. Spectra taken at varying temperatures at 2000 bar are shown in Fig. 4(A) for a portion of the spectral range 710–1275 cm^{-1}. Two prominent features appear in Fig. 4(A). A strong band corresponding to the C–OH stretching mode of the bicarbonate ion ($\nu_5(A')$) varies in frequency from 1023 cm^{-1} at 22°C to 950 cm^{-1} at 554°C. On the high frequency shoulder of this band, a second peak is found to vary from 1072 cm^{-1} at 22°C to 1049 cm^{-1} at 554°C. This band corresponds to the symmetric stretching mode ($\nu_1(A')$) of carbonate ion. Similar spectra are shown in Fig. 5(A) in which spectra collected at 554°C are given for various pressures. Additional peaks occur in Fig. 4(B) representing a portion of the 1075–1614 cm^{-1} spectral range. The narrow sharp peak near 1330 cm^{-1} is the C–C stretching mode of the diamond window of the pressure vessel. The peak varying between 1370 cm^{-1} at 22°C and 1314 cm^{-1} at 554°C represents the symmetric CO stretch ($\nu_3(A')$) of the bicarbonate ion. The spectrum shown in Fig. 6(A) taken at 22°C, 2015 bar covering the frequency interval 1075–1614 cm^{-1} shows the presence of the COH bending mode for bicarbonate ion ($\nu_4(A')$. This peak was difficult to isolate in spectra taken at higher temperatures. At temperatures above 300°C, additional peaks begin to appear at frequencies of approximately 1265, 1286, 1390, and 1410 cm^{-1}. These can be assigned to the resonance Fermi diad of carbon dioxide with the principal peaks of the diad being at $\sim$1286 and $\sim$1390 cm^{-1} with accompanying hot bands at $\sim$1265 and $\sim$1410 cm^{-1} (Dubessy et al., 1997). Resolution of these bands are more clearly shown in Fig. 5(B) where spectra taken at 554°C are presented for pressures ranging from 2014 to 1313 bar. In Fig. 6(B), a portion of a spectrum covering the third spectral range 296–889 cm^{-1} taken at 22°C, 2016 bar shows the presence of the (OH)CO and CO_2 bending modes ($\nu_7(A')$ and $\nu_6(A')$) at 641 and 679 cm^{-1}, respectively. The variations in peak positions and their half-widths for all the peaks found in the three spectral regions are shown in Fig. 2(C) and (D), respectively. As in the case of potassium carbonate solutions, Raman spectra taken both before and after the high-temperature measurements (Fig. 3(B)) indicate that the bulk solution composition remained unchanged during the experiments. A sum-

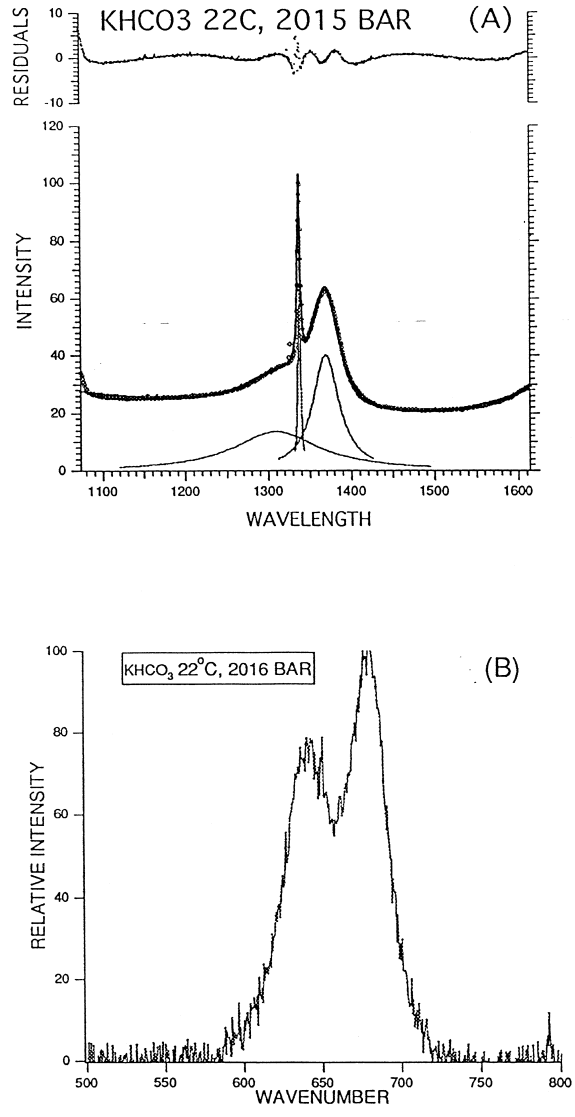

Fig. 6. Raman spectra of potassium bicarbonate. (A) Deconvoluted spectrum showing the presence of both the COH bending mode ($\nu_4(A')$) and the CO stretching mode ($\nu_3(A')$) at 22°C and 2015 bar. (B) Spectrum showing the presence of the (OH)CO and CO_2 bending modes ($\nu_7(A')$ and $\nu_6(A')$), respectively at 22°C and 2016 bar.

Table 3
Spectral parameters. One-molal potassium bicarbonate

T (°C)	Pressure (bar)	Carbonate			Bicarbonate						Carbon dioxide					
		ν_1			$\nu 5$			$\nu 3$	$\nu 7$	$\nu 6$	HB	$\nu 1'$	$\nu 1'$	HB	Mole fraction	
		Frequency	Area	FWHH	Frequency	Area	FWHH	Frequency	Frequency	Frequency	Frequency	Frequency	Frequency	Frequency	HCO_3	CO_3
2	2020	1072.4	264	18.4	1023.4	4020	30.6	1369.6	641.1	679.3	NA	NA	NA	NA	0.938	0.062
22	1524	1072.6	306	20.8	1022.6	4064	30.5	NA	NA	NA	NA	NA	NA	NA	0.930	0.070
22	1035	1071.8	252	17.4	1021.8	4164	31.1	NA	NA	NA	NA	NA	NA	NA	0.943	0.057
115	2038	1068.0	134	11.0	1009.5	3128	32.7	1360.2	633.8	676.6	NA	NA	NA	NA	0.959	0.041
114	1546	1068.4	178	10.7	1009.8	3507	33.2	1360.1	NA	NA	NA	NA	NA	NA	0.952	0.048
112	1027	1068.1	176	10.8	1008.6	3607	33.5	1359.3	NA	NA	NA	NA	NA	NA	0.953	0.047
153	2001	1067.5	192	11.1	1004.6	3380	34.4	1355.1	629.3	675.0	NA	NA	NA	NA	0.946	0.054
154	1543	1066.6	200	10.6	1003.1	3538	34.6	1355.8	NA	NA	NA	NA	NA	NA	0.947	0.053
154	1070	1066.5	199	10.6	1002.4	3468	34.3	1355.3	NA	NA	NA	NA	NA	NA	0.946	0.054
209	2035	1064.7	208	11.5	995.9	3055	36.9	1349.6	625.5	673.3	NA	NA	NA	NA	0.936	0.064
209	1528	1064.4	218	11.5	994.6	3137	37.6	1350.8	NA	NA	NA	NA	NA	NA	0.935	0.065
209	1036	1063.9	232	11.9	993.5	3143	38.1	1348.0	NA	NA	NA	NA	NA	NA	0.931	0.069
255	2022	1062.6	202	12.7	988.2	2404	39.6	1343.7	620.3	671.6	NA	NA	NA	NA	0.923	0.077
257	1497	1061.9	215	12.6	986.6	2477	39.9	1345.2	NA	NA	NA	NA	NA	NA	0.920	0.080
257	1036	1061.2	229	13.2	984.8	2521	41.2	1344.5	NA	NA	NA	NA	NA	NA	0.917	0.083
309	2021	1059.6	175	15.5	979.6	1610	42.6	1338.0	NA	NA	NA	NA	1388.9	NA	0.902	0.098
310	1511	1058.9	157	15.4	978.1	1412	43.5	1339.4	NA	NA	NA	NA	1389.2	NA	0.900	0.100
311	1014	1059.1	156	15.3	977.0	1341	44.6	1338.7	NA	NA	NA	NA	1388.4	NA	0.896	0.104
359	2013	1057.4	138	19.8	972.9	1131	46.3	1333.4	606.0	668.3	NA	NA	1390.2	NA	0.891	0.109
360	1470	1056.8	128	18.0	971.3	1103	47.8	1334.4	NA	NA	NA	NA	1389.4	NA	0.896	0.104
360	1031	1056.7	136	18.2	969.7	1115	50.0	1336.1	NA	NA	NA	NA	1389.3	NA	0.891	0.109
409	2032	1054.9	158	21.3	966.4	1212	51.5	1329.0	598.2	667.5	NA	NA	1390.4	1409.4	0.885	0.115
409	1525	1054.8	149	22.4	965.2	1038	52.9	1330.7	NA	NA	NA	NA	1389.8	1411.0	0.875	0.125
409	1059	1054.7	167	21.3	963.9	1065	54.8	1330.6	NA	NA	NA	NA	1390.0	1410.2	0.865	0.135
456	2036	1052.8	156	23.0	960.8	1079	56.9	1324.7	NA	NA	NA	NA	1391.1	1408.2	0.874	0.126
457	1545	1053.3	197	22.6	960.0	1274	59.1	1328.0	NA	NA	NA	NA	1391.0	1410.2	0.866	0.134
457	1034	1052.7	269	22.2	958.0	1337	59.7	1325.3	NA	NA	NA	NA	1391.1	1409.7	0.833	0.167
505	2043	1051.3	284	25.0	955.2	1807	62.7	1318.9	595.0	665.0	NA	NA	1390.8	1409.9	0.864	0.136
504	1530	1050.5	403	24.7	953.6	2200	65.5	1322.9	NA	NA	NA	NA	1391.1	1410.1	0.845	0.155
504	1044	1050.8	465	22.8	953.3	1793	66.5	1324.1	NA	NA	NA	NA	1391.3	1411.6	0.794	0.206
554	2014	1049.4	486	26.5	950.2	2824	69.1	1314.4	594.3	663.4	1266.2	1285.9	1391.7	1411.1	0.853	0.147
554	1710	1049.2	476	22.7	947.8	2792	68.6	1313.1	NA	NA	1264.2	1286.6	1391.4	1415.0	0.854	0.146
554	1495	1048.8	621	25.4	948.5	2974	73.9	1312.1	NA	NA	1263.8	1285.8	1391.4	1411.3	0.827	0.173
554	1313	1049.1	576	23.6	946.9	2507	74.0	1311.0	NA	NA	1264.7	1286.4	1391.2	1411.9	0.813	0.187

NA = not analyzed.
FWHH = full width at half height.

mary of the frequencies, 1/2 widths and integrated areas corresponding to these peaks for spectra taken at the various temperatures and pressures are given in Table 3.

4. Discussion

A fundamental objective of this study was to document the increased degree of formation of ion pairs and neutral species in potassium carbonate solutions with increasing temperature and decreasing density. In the case of aqueous calcium chloride, Frantz and Marshall (1982) using electrical conductivity measurements, demonstrated the two step process involving first the formation of $CaCl^+$ and then the neutral species $CaCl_2^\circ$ as a function of temperature. This can be characterized by the following equilibria:

$$Ca^{++} + Cl^- = CaCl^+ \quad (1)$$

$$CaCl^+ + Cl^- = CaCl_2^\circ \quad (2)$$

In the case of magnesium sulfate, the formation with increasing temperature and decreasing density of the neutral aqueous species $MgSO_4^\circ$ was documented using Raman spectroscopy (Frantz et al., 1994). In this study, a second band corresponding to the distorted symmetric stretching mode of the sulfate ligand in the neutral $MgSO_4^\circ$ species appeared at slightly higher frequencies than the normal stretching mode for sulfate ion. No evidence for the formation of bisulfate was recorded in this study. Determination of the relative areas of the two bands permitted calculation of their relative abundances and the mass action constant for the following equilibrium:

$$Mg^{++} + SO_4^{--} = MgSO_4^\circ \quad (3)$$

The situation is significantly different with respect to potassium carbonate solutions. If solutions containing potassium and carbonate ions behaved similarly to those containing calcium carbonate or magnesium sulfate, stepwise formation of the aqueous species KCO_3^- and $K_2CO_3^\circ$ with increasing temperature and decreasing density would be expected according to the following equilibria:

$$K^+ + CO_3^{--} = KCO_3^- \quad (4)$$

$$K^+ + KCO_3^- = K_2CO_3^\circ \quad (5)$$

The results of the present study indicate a somewhat more complicated process. The total concentration of bicarbonate (ion + ligand) is seen to dramatically increase at the expense of carbonate with increasing temperature (Fig. 7(A)) as described by the following: [1]

$$CO_3^{--} + H^+ \rightarrow HCO_3^- \quad (6)$$

No evidence is seen documenting the presence of KCO_3^-, $KHCO_3^\circ$, and $K_2CO_3^\circ$ though this may partially result from the fact that the ionic bonds responsible for the formation of 1–1 and 1–2 ion pairs are substantially weaker than those of 2–2 ion pairs like $MgSO_4^\circ$. This could result in negligible frequency shifts.

The spectra of potassium bicarbonate solutions appear to document a somewhat different trend. As temperature increases, the concentration of total carbonate increases relative to total bicarbonate according to the following (Fig. 7(B)): [1]

$$HCO_3^- \rightarrow H^+ + CO_3^{--}$$

There was no evidence of the formation of KCO_3°, $KHCO_3^\circ$, or $K_2CO_3^\circ$. Additionally, at temperatures above 300°C, aqueous carbon dioxide appears with its concentration increasing with increasing temperature and decreasing density.

4.1. Theoretical simulations

In order to understand the chemical evolution of potassium carbonate and bicarbonate fluids as they are subjected to increasing temperature and pressure, theoretical simulations of these fluids were computed using available experimentally and theoretically-determined thermodynamic data. The principal source for these data was the data base for SUPCRT92 (Johnson et al., 1992) updated with theoretically-de-

[1] This statement is based on the assumption that the trend is not just an artifact of changes in the ratio of the scattering cross-sections of carbonate and bicarbonate with increasing temperature and pressure. The validity of this assumption is discussed in Section 4.1.

rived data from Sverjensky et al. (1997). [2] Estimates of the thermodynamic properties of KCO_3^- were courtesy of D.A. Sverjensky (personal communication). Association constants for the equilibria $KCO_3^- + K^+ = K_2CO_3^\circ$ and $HCO_3^- + K^+ = KHCO_3^\circ$ were assumed to be identical to those of the equilibria $Na^+ + Cl^- = NaCl^\circ$. This is justified by the relative similarity of these constants for a variety of salts including the first association constants of $CaCl_2$ and $MgCl_2$ (Frantz and Marshall, 1982). These data were used to calculate the distributions of aqueous species for both one-molal potassium carbonate and one-molal potassium bicarbonate solutions as a function of temperature and pressure. Calculations were performed using the program listed in the Appendix of Frantz et al. (1981). Activity coefficients were computed to 300°C using the 'B-dot' equation as described in Helgeson (1969). At higher temperatures, the extended Debye–Huckel formulation was used. As the data used in these calculations of carbonate-bearing fluids is based on a paucity of experimental data, it was expected that little credence should be placed on the absolute computed concentrations. It is hoped, however, that the trends resulting from the simulations will help in understanding the results of our spectral studies.

The results of the theoretical simulation of changes in the distributions of dissolved species for K_2CO_3–H_2O fluids are shown in Fig. 8. The calculated distributions of potassium species (Fig. 8(A)) show as described by Eqs. (4) and (5) the formation of KCO_3^- followed by $K_2CO_3^\circ$ as temperature increases. Neither KOH nor $KHCO_3$ play major roles and none of the potassium bearing species can account for the rapid increase in total bicarbonate concentration with increasing temperature. The hydrogen ion concentration varies from 2.3×10^{-10} at 100°C to 7.8×10^{-10} at 550°C at a pressure of 2000 bar. In Fig. 8(B), the concentration of carbonate ions is seen to dramatically decrease with the formation of bicarbonate ions (reaction (6)) as temperature is increased. The concentration of bicarbonate ions is seen, in turn, to decrease at higher temperatures as carbon dioxide is formed. In Fig. 8(C), total concentrations of carbonate, bicarbonate, and carbon dioxide are plotted as a function of temperature. The concentration of total bicarbonate is seen to increase (though not as dramatically) relative to total carbon-

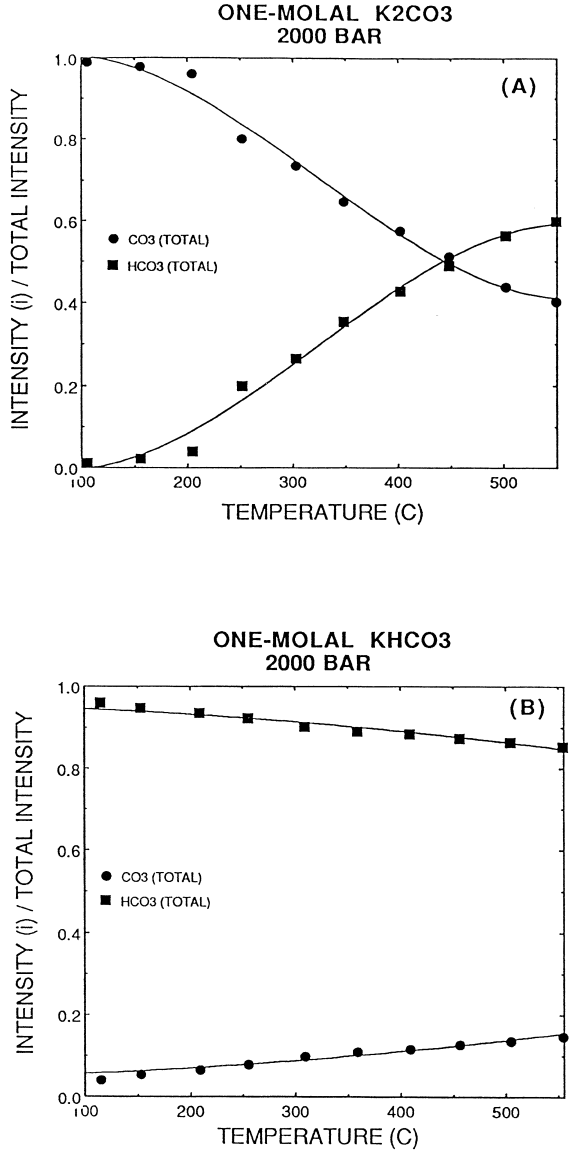

Fig. 7. Variation of the intensity of total dissolved carbonate and bicarbonate as a function of temperature at 2000 bar for (A) one molal potassium carbonate and (B) one molal potassium bicarbonate solutions.

[2] The following values were added to SUPCRT92 for KCO3$^-$: ΔG (−194451.0); ΔH (−224105); S (17.9); V (8.5); C_p (−16.0); a_1 (34.414); a_2 (0.006244); a_3 (5.4970); a_4 (−0.00028); c_1 (9.2288); c_2 (−0.000063); Omega (0.00000136).

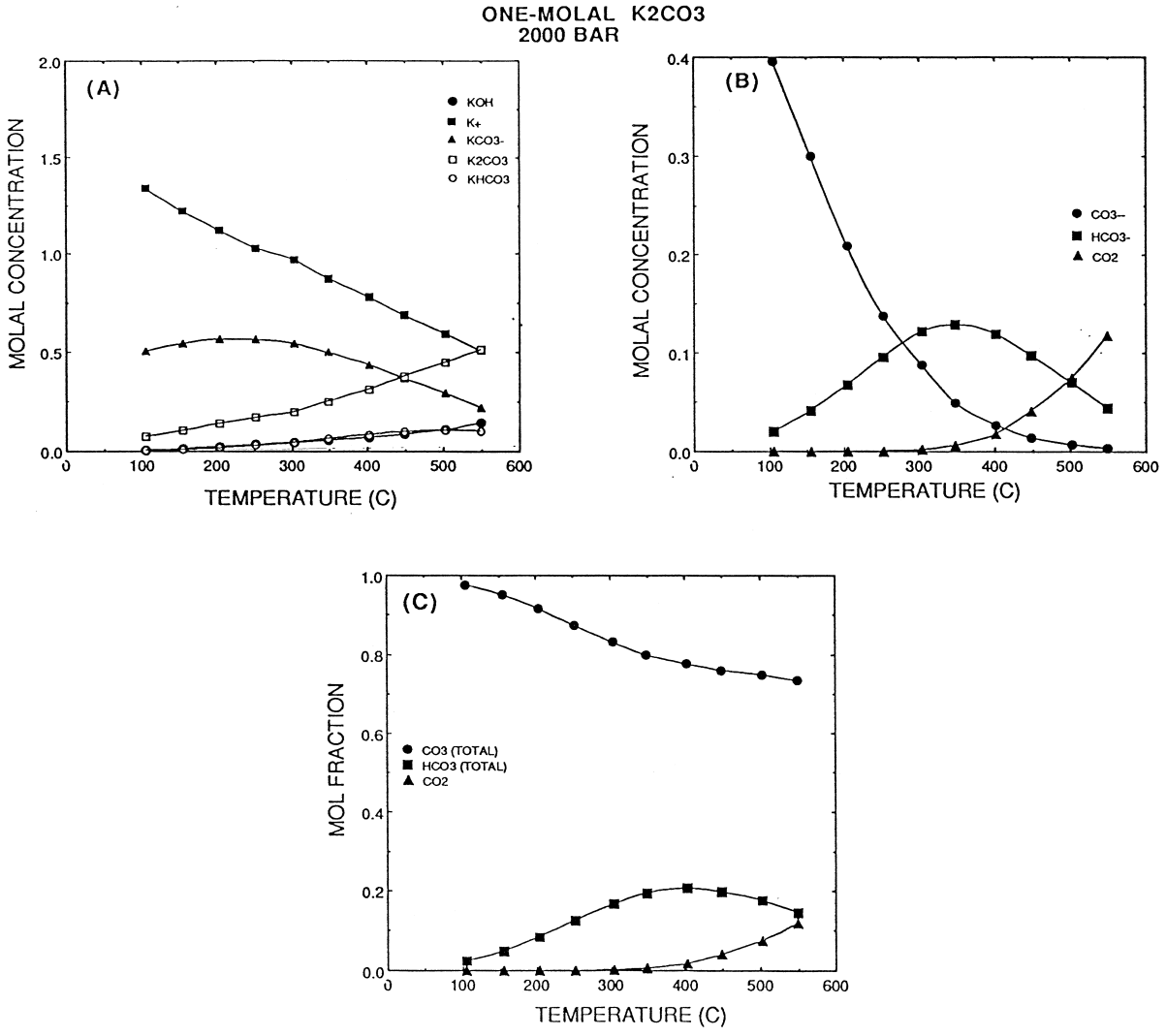

Fig. 8. Variation of the concentration of dissolved solutes in one-molal potassium carbonate solutions as a function of temperature at 2000 bar. (A) Molality of potassium bearing species. (B) Molality of carbonate ion, bicarbonate ion, and aqueous carbon dioxide. (C) Mole fraction of *total* dissolved carbonate, bicarbonate, and aqueous carbon dioxide.

ate as do the relative intensities of total CO_3 and total HCO_3 in our spectral study (Fig. 7(A)). This is due to the formation of bicarbonate ions at the expense of carbonate ions thus inhibiting the degree of formation of KCO_3^- and $K_2CO_3^\cdot$.

In theoretical simulations of $KHCO_3$–H_2O fluids, changes in the distributions of dissolved species as a function of temperature follow a somewhat different path. The principal carbon-bearing potassium complexes at lower temperatures are $KHCO_3$ and KCO_3^- (Fig. 9(A)). As temperature increases, however, the concentration of $K_2CO_3^\cdot$ increases becoming dominant above 500°C. The hydrogen ion concentration changes from 1.9×10^{-7} at 100°C to 1.4×10^{-9} at 550°C at 2000 bar. Changes in the distribution of the concentrations of the carbonate, bicarbonate, and aqueous carbon dioxide complexes follow the same trend as in the case of KCO_3–H_2O solutions (Fig. 9(B)). The concentration of carbonate ions steadily decreases with increasing temperature; bicarbonate,

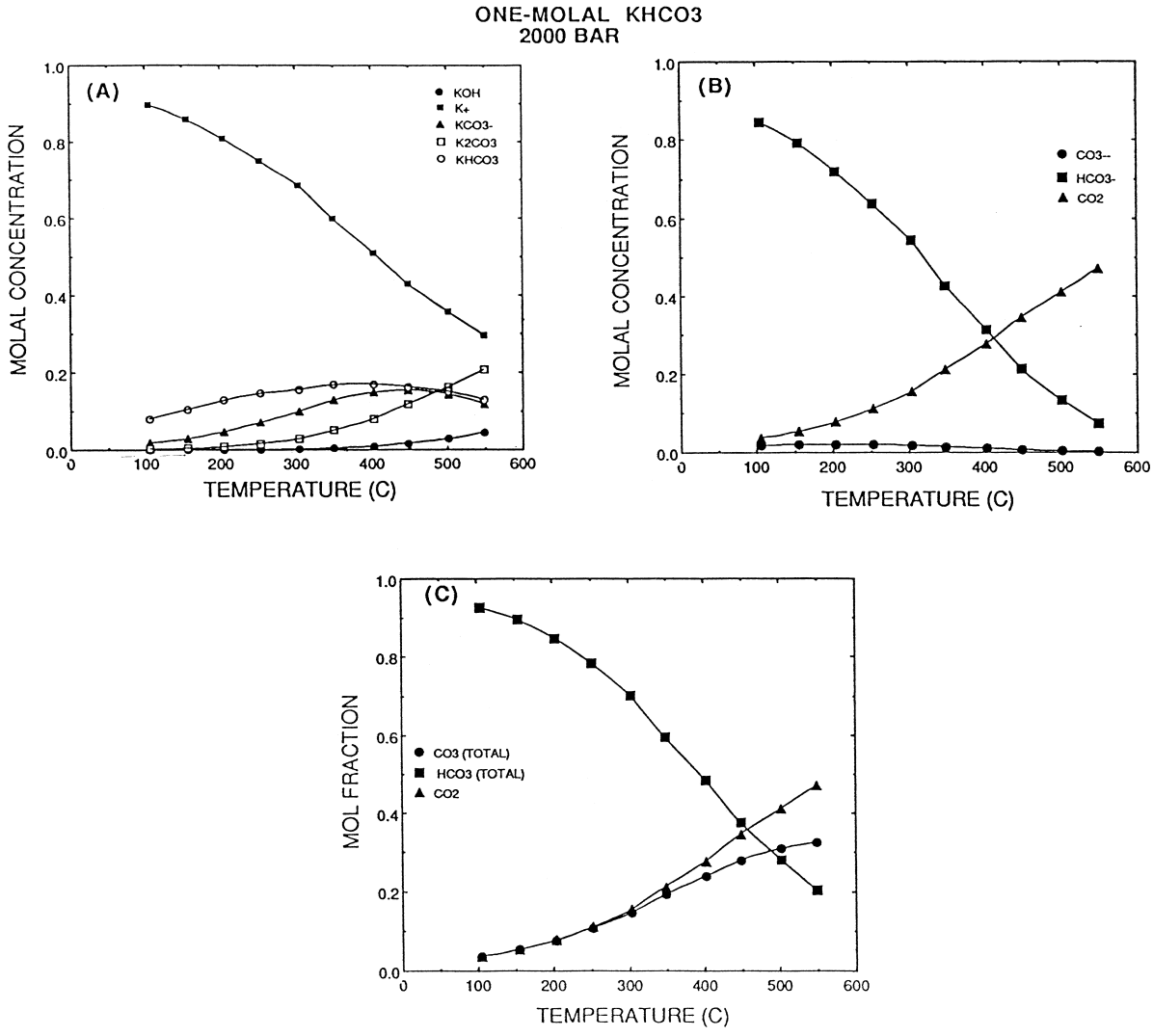

Fig. 9. Variation of the concentration of dissolved solutes in one-molal potassium bicarbonate solutions as a function of temperature at 2000 bar. (A) Molality of potassium bearing species. (B) Molality of carbonate ion, bicarbonate ion, and aqueous carbon dioxide. (C) Mole fraction of *total* dissolved carbonate, bicarbonate, and aqueous carbon dioxide.

the predominant carbonate ion at room temperature also monotonically decreases with increasing temperature as the concentration of dissolved carbon dioxide increases. The overall distribution of total carbonate, bicarbonate and carbon dioxide in Fig. 9(C) predicts an increase in the concentration of total carbonate at the expense of total bicarbonate with increasing temperature. This is primarily due to the formation of significant concentrations of K_2CO_3. Also predicted is the appearance of aqueous carbon dioxide at higher temperatures. These trends are both documented in the spectral investigations (Fig. 7(B) Fig. 4(A)Fig. 5(B)).

The relative peak areas representing total dissolved carbonate and bicarbonate given in Table 2 and Fig. 7(A) for one-molal K_2CO_3 and in Table 3 and Fig. 7(B) for one-molal $KHCO_3$ can be related to the theoretically calculated distributions of total carbonate and bicarbonate shown for these solutions in Fig. 8(C)Fig. 9(C). This can be accomplished by

considering the following relationship between species concentration and the intensity of its Raman peak:

$$I_i = \gamma_i C_i \quad (8)$$

where I_i is the intensity of the peak representing the ith species; C_i is the concentration of species i in molarity; and γ_i is the scattering coefficient of the ith species. Considering the ratio of the intensities of two species, Eq. (8) becomes:

$$I_1/I_2 = (\gamma_1/\gamma_2)(C_1/C_2) \quad (9)$$

Assuming: (1) peak area ratios are proportional to peak intensities; (2) the scattering efficiency of all carbonate species are equal; and (3) the scattering efficiency of all bicarbonate species are equal,

$$A_{\text{carb}}/A_{\text{bicarb}} = \Gamma(m_{\text{carb}}/m_{\text{bicarb}}) \quad (10)$$

where A_{carb} is the area under the peak representing total carbonate; A_{bicarb} is the area under the peak representing total bicarbonate; Γ is the ratio of the scattering coefficients; and m_{carb} and m_{bicarb} represent the molal concentrations of total carbonate and bicarbonate, respectively. Using the data for the total carbonate and bicarbonate peak areas in Tables 2 and 3 for the K_2CO_3 and $KHCO_3$ solutions in conjunction with the total computed concentrations representing the various carbonate and bicarbonate species (shown in Fig. 8(C) and Fig. 9(C), respectively), values of the ratio of the scattering coefficients Γ have been be computed for each of the two solutions. If the previously-stated assumptions and the theoretical simulations of species distributions are correct, the scattering coefficient ratios for both solutions should be identical at fixed temperature and pressure. As seen in Fig. 10 for solutions at 2000 bar, they are surprisingly close considering the inherent errors in the computations. The ratio of the scattering coefficient of carbonate to bicarbonate is seen to decrease with increasing temperature which may not be surprising considering the large differences in the temperature dependence of both their frequencies and half-widths with increasing temperature. The pressure dependence of this ratio is undetectable in the calculations.

The calculations of scattering coefficient ratios lends credence to the theoretical calculations of species distributions at elevated temperatures and pressures. Not only do the temperature-dependent trends demonstrated by comparison of Fig. 7(A),(B) with Fig. 8(C)Fig. 9(C) agree, but the actual ratios of concentrations of the computed species distributions agree with observed Raman measurements (as demonstrated in Fig. 10). The apparent differences between these two sets of figure are reconciled by the cross-sectional differences of the Raman scattering. The results thus indirectly verify the presence of the potassium carbonate and bicarbonate ion pairs.

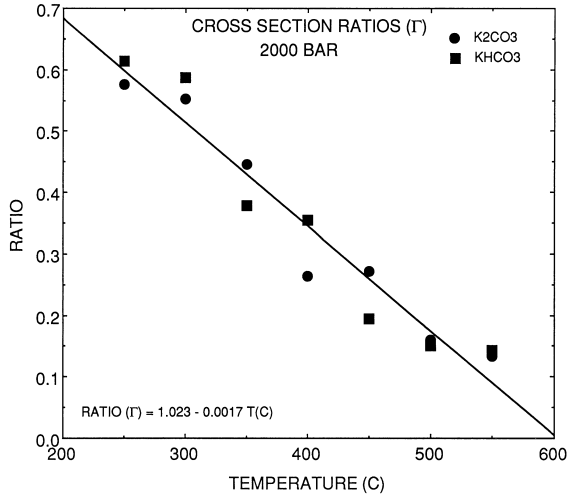

Fig. 10. Variation of the Raman scattering coefficient ratio (Γ) of total carbonate as a function of temperature at 2000 bar. The filled circles represent ratios calculated for one-molal potassium carbonate solutions; the filled squares, for one-molal potassium bicarbonate solutions. The line represents a least-squares fit to all the data.

5. Conclusions

The behavior of complicated systems under hydrothermal conditions such potassium carbonate solutions are poorly known due to the lack of experimentally-derived data. Characterization requires the *simultaneous* determination of numerous mass action constants. Current efforts are focusing on theoretical estimates of the thermodynamic properties of dissolved species of complicated systems such as this (i.e., Sverjensky et al., 1997). The experimental bases for many of the predictions, however, are frequently lacking. In the case of hydrothermal fluids containing potassium carbonate and potassium bicarbonate,

spectroscopic investigations of the presence and relative intensities of peaks representing total dissolved carbonate, bicarbonate, and aqueous carbon dioxide support the trends which can be predicted by theoretical simulations. The interplay between theoretical prediction of speciation in complicated hydrothermal fluids and the monitoring of the presence and relative abundance of dissolved species in experimental fluids using spectroscopic measurements should be a constructive avenue in furthering our knowledge of supercritical fluids.

Acknowledgements

The author is indebted to B.O. Mysen, D.A. Sverjensky, R. Arvidson, E. Oelkers, S. Lvon, and F.T. Mackenzie for their assistance. The project was supported by the Carnegie Institution of Washington and a grant from the Centre National de la Recherche Scientifique through its Programme International de Cooperation Scientifiique (PICS #142).

References

Colthup, N.B., Daly, L.H., Wiberley, S.E., 1975. Introduction to Infrared and Raman Spectroscopy. Academic Press, New York, 523 pp.

Davis, A.R., Oliver, B.G., 1972. A vibrational-spectroscopic study of the species present in the CO_2–H_2O system. J. Solution Chem. 1 (4), 329–338.

Dubessy, J., Moissette, A., Bakker, R., Frantz, J.D., Zhang, Y.-G., 1997. High temperature Raman spectroscopic study of H_2O–CO_2–CH_4 mixtures in synthetic fluid inclusions: first insights on molecular interactions and analytical implications. Eur. J. Mineral., in review.

Eugster, H.P., Skippen, G.B., 1967. Igneous and metamorphic reactions involving gas equilibria. In: Abelson, P.H. (Ed.), Researches in Geochemistry. Wiley, New York, pp. 492–520.

Frantz, J.D., 1981. High-pressure, high-temperature optical cell for Raman spectroscopy. Carnegie Institution of Washington Yearbook 80, 406–408.

Frantz, J.D., Marshall, W.L., 1982. Electrical conductance and ionization constants for calcium chloride and magnesium chloride in aqueous solutions at temperatures to 600°C and pressures to 4000 bar. Am. J. Sci. 282, 1666–1693.

Frantz, J.D., Popp, R.K., Boctor, N.Z., 1981. Mineral-solution equilibria: V. Solubilities of rock-forming minerals in supercritical fluids. Geochim. Cosmochim. Acta 45 (1), 69–77.

Frantz, J.D., Dubessy, J., Mysen, B.O., 1993. An optical cell for Raman spectroscopic studies in supercritical fluids and its application to the study of water to 500°C and 2000 bar. Chem. Geol. 106, 9–26.

Frantz, J.D., Dubessy, J., Mysen, B.O., 1994. Ion-pairing in aqueous $MgSO_4$ solutions along an isochor to 500°C and 11 kbar using Raman spectroscopy in conjunction with the diamond-anvil cell. Chem. Geol. 116, 181–188.

Greenwood, H.J., 1969. The compressibility of gaseous mixtures of carbon dioxide and water between 0 and 500 bar pressure and 450° and 800°C. Am. J. Sci. A 267, 191–208.

Greenwood, H.J., 1973. Thermodynamic properties of gaseous mixtures of H_2O and CO_2 between 450° and 800°C and 0 to 500 bar. Am. J. Sci. 273, 191–208.

Helgeson, H.C., 1969. Thermodynamics of hydrothermal systems at elevated temperatures and pressures. Am. J. Sci. 267, 729–804.

Holloway, J.R., 1984. Graphite–CH_4–H_2O–CO_2 equilibria at low-grade metamorphic conditions. Geology 12, 455–458.

Johnson, J.W., Oelkers, E.H., Helgeson, H.C., 1992. SUPCRT92: a software package for calculating the standard molal thermodynamic properties of minerals, gases, aqueous species, and reactions from 1 to 5000 bar and 0 to 1000°C. Computers and Geosciences 18 (7), 899–947.

Kerrick, D.M., Jacobs, G.K., 1981. A modified Redlich–Kwong equation for H_2O, CO_2 and H_2O–CO_2 mixtures at elevated pressures and temperatures. Am. J. Sci. 281, 735–767.

Kruse, R., Franck, E.U., 1982. Raman spectra of hydrothermal solutions of CO_2 and HCO_3 at high temperatures and pressures. Ber. Bunsenges Phys. Chem. 86, 1036–1038.

Oliver, B.G., Davis, A.R., 1973. Vibrational spectroscopic studies of aqueous alkali metal bicarbonate and carbonate solutions. Can. J. Chem. 51, 698–702.

Saxena, S.K., Fei, Y., 1988. Fluid mixtures in the C–H–O system at high pressure and temperature. Geochim. Cosmochim. Acta 52, 505–512.

Sverjensky, D.A., Shock, E.L., Helgeson, H.C., 1997. Prediction of the thermodynamic properties of aqueous metal complexes to 1000°C and 5 kb. Geochim. Cosmochim. Acta 61 (7), 1359–1412.

Zhang, Y.-G., Frantz, J.D., 1989. Experimental determination of the compositional limits of immiscibility in the system $CaCl_2$–H_2O–CO_2 at high temperatures and pressures using synthetic fluid inclusions. Chem. Geol. 74, 289–308.

Zhang, Y.-G., Frantz, J.D., 1992. Hydrothermal reactions involving equilibrium between minerals and mixed volatiles: 2. Investigations of fluid properties in the CO_2–CH_4–H_2O system using synthetic fluid inclusions. Chem. Geol. 100, 51–72.